Crack initiation mechanisms in torsional fatigue

Véronique Doquet

CRACK INITIATION MECHANISMS IN TORSIONAL FATIGUE

V. DOQUET
Laboratoire de Mécanique des Solides, URA CNRS 317, Ecole Polytechnique, 91128 Palaiseau cedex, France

Abstract—The development of fatigue damage in Co45Ni specimens during push–pull and reversed torsion tests, performed inside a scanning electron microscope, was observed and the different stress states compared. It appeared that transgranular crack initiation and development is delayed and intergranular crack initiation promoted under torsional loading. This was explained in terms of reduced surface distortion at the emergence of persistent slip bands (PSBs) and smaller compatibility stresses at the PSB-matrix interfaces. The influence of the mechanical strength of grain boundaries on the difference between tensile and torsional fatigue lives is discussed.

Keywords—Torsional fatigue; Intergranular crack initiation

INTRODUCTION

Searching for a fatigue criterion suitable for multiaxial loadings, many authors have found that under equal von Mises equivalent plastic strain ranges, the lifetime of thin tubular specimens is larger under reversed torsion than under push–pull for a wide variety of materials [1–5]. The ratio between torsional and tensile fatigue lives reported for various FCC and BCC alloys is drawn as a function of von Mises equivalent plastic strain range in Fig. 1. This ratio appears to rise as the strain range, $\Delta\varepsilon_{p.eq}$, decreases. Since stage I represents a portion of the fatigue life that also increases as $\Delta\varepsilon_{p,eq}$ decreases, this suggests that the discrepancy between fatigue lives originates from a longer stage I phase under reversed torsion. Two reasons were invoked to explain this.

First, Brown and Miller [6] and then Lohr and Ellison [7] considered the maximum shear strain $(\varepsilon_I - \varepsilon_{III})/2$ (where $\varepsilon_I \geqslant \varepsilon_{II} \geqslant \varepsilon_{III}$ denote the principal strains) to be the driving force for fatigue crack initiation. When this shear strain acts parallel to the surface (case A) this is less detrimental than when it is normal at the surface (case B). In the former case, a shallow crack will develop along the surface whereas in the latter, it will grow inwards. Actually, the cracks developed under torsional loading (which pertains to case A, Fig. 2(a)) have a much smaller depth to length ratio than those generated by tensile loading (which pertains to both cases since ε_{II} is then equal to ε_{III} Fig. 2(b)) [8].

Second, even though the reversed shear strain is recognized as the driving force for fatigue crack initiation, the presence of an opening stress on highly sheared facets is considered to assist the development of microcracks and their transition to stage II. The absence of such an opening stress for torsional loading could thus explain the longer stage I phase during which microcracks grow in pure mode II, compared to the tensile case where they grow in mixed mode I and II. In fact, the most popular fatigue criteria proposed by Fatemi and Socie [9] and Brown and Miller [6] incorporate both the maximum shear strain range and the stress (or strain) normal to the facets that undergo the maximum shear strain range. The relative importance of the second term has to be adjusted through material constants, so as to unify the tensile and torsional fatigue data. The efficiency of these criteria is not questioned here, but further questions remain about the relationship between the material constants and microstructure since, as it can be seen on Fig. 1, the difference

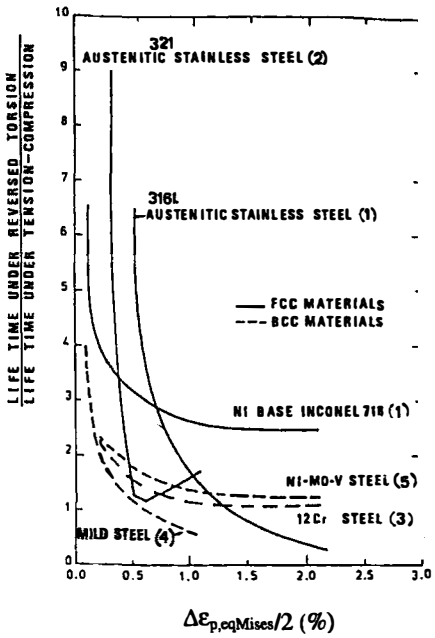

Fig. 1. Comparison between fatigue lives under push–pull and reversed torsion for various materials.

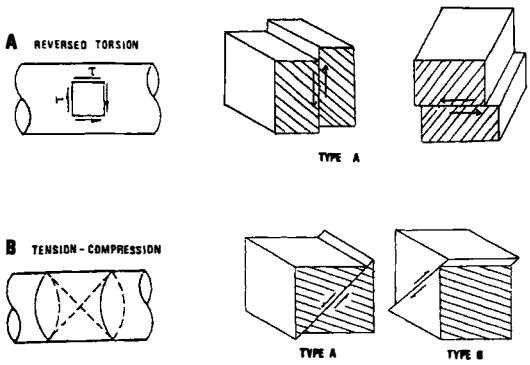

Fig. 2. Orientation of maximum shear strain facets for (A) reversed torsion, (B) push–pull; (the external surface is hatched).

between tensile and torsional fatigue lives is very pronounced for some alloys, especially low stacking-fault energy austenitic steels (in which it can reach an order of magnitude), and not so important for other materials. It is thus thought that purely mechanical reasons do not entirely explain these differences that could perhaps be caused from different crack initiation mechanisms under torsional loading. Therefore, fatigue crack initiation mechanisms and damage development kinetics observed during push–pull and reversed torsion tests, performed here on an austenitic alloy, are compared and discussed in the present paper.

EXPERIMENTAL OBSERVATIONS

Procedures

The development of fatigue damage at the surface of thin tubular specimens (10.8 mm outer diameter, 0.9 mm wall thickness, 170 mm gauge length) of Co45Ni alloy was observed during push–pull and reversed torsion tests carried out on a specially designed biaxial loading frame able to work inside the chamber of a scanning electron microscope [10]. The material has a %wt. composition of 45.0 Ni, 0.009 C, <0.001 S, 0.01 Mg, 0.002 Mn, 0.014 Si, 0.015 Al and the balance Cobalt. It is a FCC solid solution with a stacking-fault energy (SFE) of 45 mJ/m^2 and an average grain size of 25 μm. Its yield stress, ultimate tensile stress and elongation to fracture are 170 MPa, 560 MPa and 71% respectively at room temperature. For comparison, similar tests performed on a Co33Ni alloy (that differs from the present material mainly in its SFE (15 mJ/m^2)) should throw some light on the influence of the SFE on multiaxial fatigue damage development.

Before the tests, square metallic microgrids with a 5 μm mesh size were laid on the electropolished surface of the specimens, covering 7 or 8 areas of 1 mm^2 each and these were systematically inspected each time the tests were interrupted.

The tensile and torsional tests were run under displacement and rotation control with frequencies of 0.025 and 0.066 Hz respectively. Note that vacuum was established only during observations, the tests themselves being performed in laboratory air. The displacement and rotation amplitudes were adjusted so that, at steady-state, approximately equal von Mises equivalent stress ranges were reached:

$$\frac{\Delta\sigma}{2} = 322 \text{ MPa}, \quad \sqrt{3}\frac{\Delta\tau}{2} = 343 \text{ MPa}$$

which, according to the cyclic stress–strain curve established by previous conventional tests [11], corresponds to an equivalent plastic strain range: given by $\Delta\varepsilon_{p,eq}/2 = \Delta\gamma_p/2\sqrt{3} \approx 0.17\%$. Tests were stopped when a microscopic crack was formed, that is after 5530 cycles for reversed torsion and 1900 cycles for push–pull (the latter seemed somewhat premature compared to previous data but this does not invalidate the observations reported below concerning crack initiation). The ratio between the torsional and tensile fatigue lives (2.9) is markedly lower than those reported in Fig. 1 for some other FCC materials at the same plastic strain range. But, as discussed below, there are too many microstructural parameters likely to influence this ratio (grain boundaries mechanical strength, grain size, SFE, precipitates) when making general conclusions from so many different materials.

Observations

During torsional testing, some distortion of the microgrids appeared, early in the fatigue life, and built up gradually as a result of irreversible dislocation glide parallel to the free surface. After a few hundred cycles, some of the longitudinal lines of the grids crossed by transverse slip bands had undergone transverse displacements of 0.4 to 1 μm. The local shear strain accumulated in these glide bands- or, more precisely its component on the surface plane-estimated as the ratio between the transverse displacement and the band thickness (about 2 μm), ranged from 20 to 50% (Fig. 3(a)). The distortion was also particularly clear near grain boundaries where slip intensifies to ensure strain compatibility between neighbouring grains (Fig 3(b)).

In a few grains, probably where the Burgers vector of the activated slip system was not perfectly parallel to the surface, intrusions and extrusions were seen and after 6% of the lifetime, i.e. 320 cycles, transgranular microcracks seemed to have initiated along some portions of the PSBs of

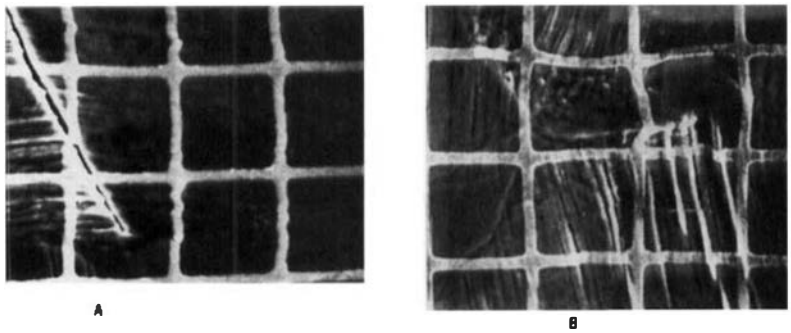

Fig. 3. Aspects of microgrids during a torsional test. (A) Localized distortion of the microgrids after 1000 cycles. (B) Distortion of the microgrids at a grain boundary after 600 cycles (the pitch of the grids is 5 μm).

these grains. But this type of damage was marginal and developed slowly: the first observation of a transgranular microcrack that had developed into a neighbouring grain was at 3500 cycles.

At 11% of the lifetime (600 cycles) cavities were nucleated along grain and annealing twin boundaries by intense slip bands impinging on them at a high angle, generally ranging from 70 to 90 degrees (Fig. 4(a)) and from them, intergranular microcracks developed (Fig. 4(b)). They constituted a roughly longitudinal and transversal network that intensified up to a point where the mean distance between microcracks was of the order of one or two grain diameters (Fig. 5), and where coalescence was frequent. In spite of this large number of microcracks, the load range did not drop significantly up to 99% of the fatigue life, which is consistent with the low average depth of the microcracks measured along longitudinal sections after the test (38 μm).

At 99% of the fatigue life, a transverse crack, several millimeters long, was observed, and pictures were made at maximum and minimum rotation angle (Fig. 6(a), (b)). From these pictures, it can be understood how the specimen sustained the full torque range: the load was transmitted through the asperities of the crack flanks which came into contact. After 130 additional cycles, these

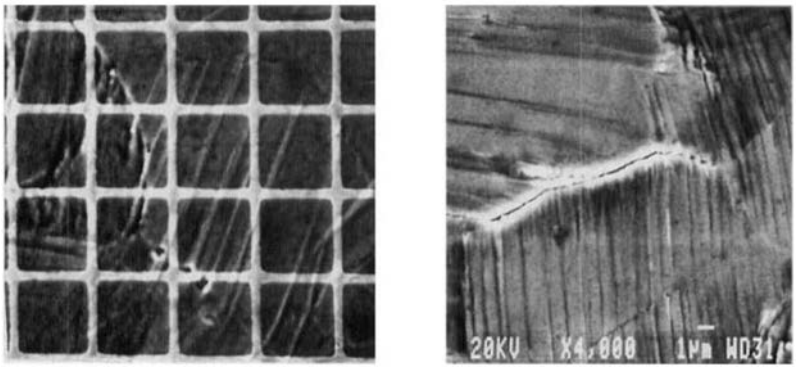

Fig. 4. Damage development during a torsional test. (a) Slip-induced cavitation of a grain boundary after 600 cycles, (b) intergranular microcrack (the pitch of the grids is 5 μm and the axis of the specimen is vertical). Both photographs are at the same magnification.

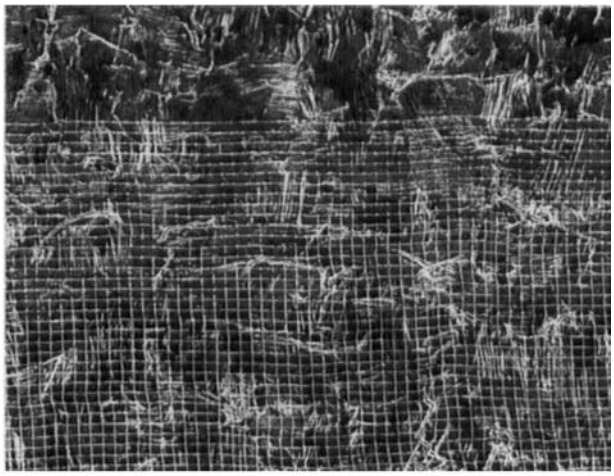

Fig. 5. The network of microcracks after 5000 torsional cycles (the pitch of the grids is 5 μm and the axis of the specimen is vertical).

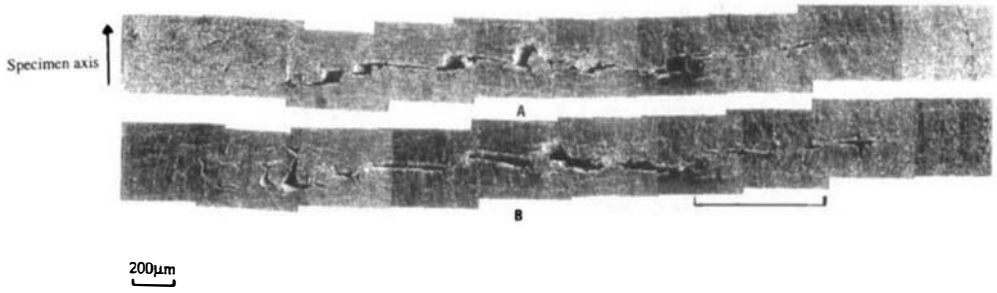

Fig. 6. The main crack after 5500 torsional cycles at (A) maximum and (B) minimum rotation angle (the bar in (B) shows the portion of the crack that is enlarged in Fig. 9).

asperities were completely worn away due to alternating mode II + III crack flank displacements (Fig. 7) and the load-bearing capacity of the specimen had dropped by more than 70%.

Due to the sliding wear of fracture surfaces, fractographic observations do not bring any useful information, neither concerning the main crack initiation mode, nor the proportion of trans- or intergranular-fracture.

The tortuous path of the crack and the presence, along its flanks, of numerous square-shaped particles, 20 to 50 μm in size (Fig. 8) strongly suggest a contribution of microcrack coalescence events to the development of the main crack. As additional evidence, a close examination of Fig. 6 shows that, at this stage, the crack located on the right hand side is not yet connected to the main crack whereas 130 cycles later it is (Fig. 9). The coalescence process seems to take place rather quickly and late in the fatigue life which would thus mainly depend on the crack initiation kinetics.

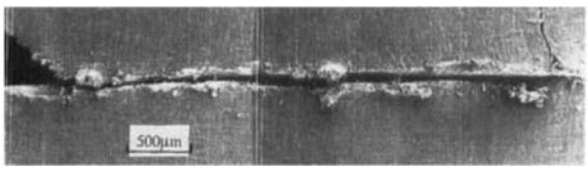

Fig. 7. A part of the main crack after 5630 torsional cycles.

Fig. 8. Debris along the main crack flanks during a torsional test.

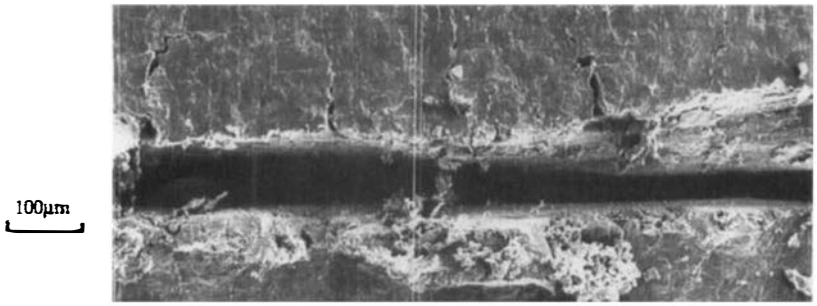

Fig. 9. Detail of the main crack at 5630 torsional cycles which corresponds to the zone marked by a bar on Fig. 6(B).

During the push–pull test, some distortion of microgrids was observed only within a few grains for which the Burgers vector of the activated slip system probably had a large component parallel to the surface. In these grains, slip line traces were approximately 45° to the axis of the specimen, which is consistent with the orientation of type A facets in push–pull.

In a large majority of the grains, very little distortion was observed, but extrusions and intrusions started to form after 55 cycles and developed rather quickly (compare Fig. 10(a), (b) and (c)), leading to transgranular microcrack initiation around 155 cycles. After 1650 cycles, some of these microcracks began to grow beyond the first grain boundary to be encountered. A few microcracks were also initiated along annealing twin boundaries. Intergranular crack initiation was marginal and mainly affected the boundaries of grains where the distortion of the microgrids was significant.

DISCUSSION

Crack initiation

Intergranular crack initiation has long been known to occur under high strain–low-cycle fatigue as a result of a notch effect at boundaries where grain-to-grain differences in out-of-surface displacement are important [12].

The push–pull test carried out here at a strain level equivalent to that of the torsion test has shown that this strain level is not sufficient to induce such a phenomenon. Anyway, the specimen submitted to the torsional test does not exhibit any surface rumpling.

No environmental effect can be invoked to explain intergranular crack initiation since the torsional test was carried out in laboratory air and at a higher frequency that its tensile counterpart.

The observed tendency for intergranular initiation under torsional fatigue thus stems from the loading mode.

A similar fact is reported for 316L stainless steel by Jacquelin [1] and is also mentioned by Socie [13]. In a previous study [4], in-phase tension and torsion biaxial fatigue tests were carried out on a mild steel (BCC structure) for various proportions of each loading mode. The frequency of intergranular crack initiation, reported in Table 1, was observed to increase with the proportion of torsional loading for roughly similar Von Mises equivalent stress ranges. The effect was however less pronounced than in the present study.

In fact, both the theoretical model of Tanaka and Mura [14] and that of Mughrabi [15], which was sustained by experimental evidence obtained on polycrystalline copper loaded in push–pull

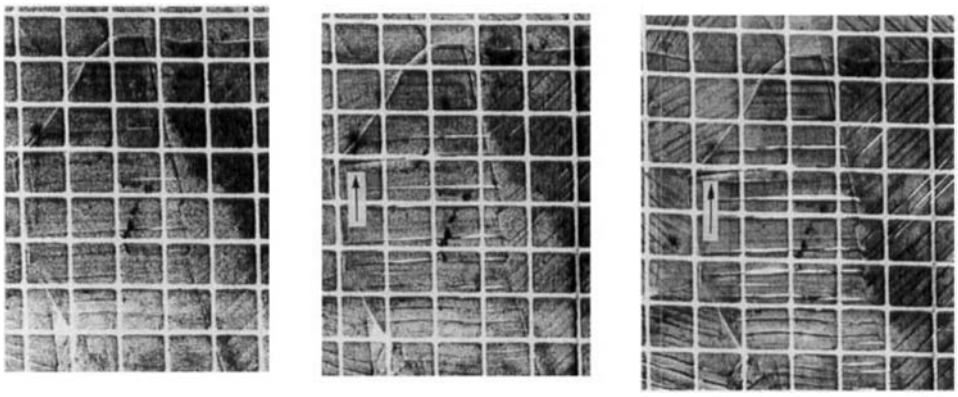

Fig. 10. Damage development during a push–pull test. The same zone observed after (a) 55, (b) 255 and (c) 855 cycles, the microcrack is arrowed and the pitch of the grids is 5 μm.

Table 1. Frequency of intergranular microcracks observed at the surface of mild steel specimens after in-phase tension and torsion cyclic tests [4]. The parameter λ is the ratio between the imposed shear strain $\Delta\gamma$ and the axial strain $\Delta\varepsilon$

λ	0	1.9	2.2	∞
$\frac{\Delta\sigma_{eq,Mises}}{2}$ (MPa)	171	144	165	189
percentage of intergranular microcracks	26%	35%	45%	45%

[16], predict intergranular crack initiation under high cycle fatigue, due to PSB–GB interactions, when the Burgers vector of gliding dislocations in one of the adjacent grains is parallel to the surface. The fact that under torsional loading, this situation is much more frequent than under push–pull partly explains the change in the crack initiation mode observed here.

Another part of the explanation probably lies in a delay of transgranular crack initiation when the out-of-surface component of the Burgers vector is small and the relief associated with PSBs is thus limited. The first transgranular microcracks were observed here after 320 cycles under reversed torsion compared to 155 cycles under push–pull.

In the same way, Jacquelin [1] observed that type A microcracks were less numerous than type B in 316L and Inconel 718 tubular specimens tested in push–pull, a case where loading on both type of facets is equal. Furthermore, this was also true with a superimposed internal pressure, in spite of higher normal and shear stresses on type A facets in this case. Recent work on aluminium single crystals has shown that tiny fatigue cracks can initiate (perpendicular to the PSBs) on the surface that contains the active Burgers vector, in the absence of any intrusions, extrusions or protrusions [17]. But even though the notch effect associated with slip-induced surface roughening is not the only origin of transgranular crack initiation, it is clear that it will promote the event.

Compatibility stresses at the PSB-matrix interface can also be considered as a possible origin for transgranular crack initiation. Deperrois [18] has calculated the tensile stress singularity at the interface between a plastically deformed inclusion emerging at the free surface of a semi-infinite elastic matrix and this matrix. He compared the cases were the plastic strain in the inclusion pertains to case A and B and found that the tensile singularity is smaller (by a factor of ν, the Poisson's ratio) in the former case. So, this point of view would also lead to the conclusion that torsional loading is less favorable than push–pull to transgranular crack initiation.

Concerning the intrinsic and extrinsic factors that determine the relative resistance of a material to tensile and torsional fatigue, it is clear that the parameters likely to modify the relative mechanical strength of grain boundaries and bulk material (such as the presence of segregated impurities, the heat treatment and the environment) will be important. A high strength of grain boundaries will probably enlarge the difference between tensile and torsional fatigue lives in the range of high-cycle fatigue (except if intergranular crack initiation already predominates under push–pull).

Additionally an influence of the grain size is likely to exist: according to Mughrabi [15], a large grain size promotes intergranular crack initiation. It could thus reduce the difference between tensile and torsional fatigue lives at small strain ranges.

Development of microcracks

Under reversed torsion, not only the initiation of transgranular microcracks was delayed but also their development into a neighbouring grain which was first observed after 3500 cycles instead of 1650 cycles under push–pull. This delay could arise either from a slower propagation rate towards the grain boundary in the absence of an opening stress or from an increased difficulty for a pure shear microcrack to overcome a grain boundary.

Further observations will be performed to clarify this point. If the latter explanation prevails this would give an even greater importance to the strength of grain boundaries in relation to the resistance of the material to torsional fatigue.

Note that, contrary to transgranular microcracks that are mainly mode II cracks, some of the intergranular microcracks (those that originate from a glide band impinging on the GB with an angle less than 90°) are submitted to mixed shear and opening conditions. This could explain why they seem to develop more easily than their transgranular counterparts.

CONCLUSIONS

Compared to push–pull, torsional cyclic loading tends to delay transgranular crack initiation. This is attributed to a reduced surface distortion at the emergence of PSBs and smaller compatibility stresses at PSB–matrix interfaces.

Transgranular microcrack development beyond the first grain boundary is also delayed under reversed torsion. The reason for this delay has to be clarified in terms of either slower micro-crack propagation rate in the absence of an opening stress or increased difficultly in overcoming the grain boundary for a pure shear microcrack.

Torsional cyclic loading also tends to promote intergranular crack initiation.

For a given material, the preferred crack initiation mode in torsional fatigue should depend on the relative strength of grain boundaries and bulk material and this should also influence fatigue endurance in the high-cycle regime.

An attempt to vary the mechanical strength of grain boundaries in a given alloy through controlled segregation or precipitation is required.

REFERENCES

1. B. Jacquelin (1983) Amorçage des fissures en fatigue oligocyclique sous chargement multiaxial. Ph.D. Thesis, Ecole des Mines de Paris.
2. C. M. Sonsino and V. Grubisic (1985) Fatigue behavior of cyclically softening and hardening steels under multiaxial elastic-plastic deformation. In: *Multiaxial Fatigue*, ASTM STP 853 (Edited by K. J. Miller and M. W. Brown), pp. 586–605. American Society for Testing Materials, Philadelphia.
3. M. Robillard (1989) Etude de l'endommagement et de la rupture en fatigue oligocyclique multiaxiale. Ph.D. Thesis, Ecole des Mines de Paris.
4. V. Doquet and A. Pineau (1991) Multiaxial low-cycle fatigue behaviour of a mild steel. In: *Fatigue Under Biaxial and Multiaxial Loading* ESIS 10 (Edited by K. Kussmaul and D. McDiarmid), pp. 81–101. MEP, London.
5. R. A. Williams, R. J. Racek, O. Klufas, S. Adams and D. C. Gonyea (1985) Biaxial torsional fatigue of turbine generator rotor steels. In: *Multiaxial Fatigue*, ASTM STP 853 (Edited by K. J. Miller and M. W. Brown), pp. 135–152. American Society for Testing Materials, Philadelphia.
6. M. W. Brown and K. J. Miller (1973) A theory for fatigue failure under multiaxial stress–strain conditions. *Proc. Inst Mech. Engrs* **187,** 65–73.
7. R. D. Lohr and E. G. Ellison (1980) A simple theory for low-cycle multiaxial fatigue. *Fat. Engng Mater. Struct.* **3,** 1–17.
8. C. T. Hua and D. F. Socie (1984) Fatigue damage in 1045 steel under constant amplitude biaxial loading. *Fat. Engng Mater. Struct.* **7,** 165–179.

9. A. Fatemi and D. F. Socie (1988) A critical plane approach to multiaxial fatigue damage including out-of-phase loading. *Fat. Fract. Engng Mater. Struct.* **11,** 149–165.
10. V. Doquet, D. Caldemaison and T. Bretheau (1995) Combined tension and torsion cyclic tests inside a scanning electron microscope. *Proc. 4th Int. Conf. on Biaxial and Multiaxial Fatigue*, May 31–June 3, Saint-Germain-en-Laye, France, pp. 19–26.
11. V. Doquet and M. Clavel (1996) Stacking-fault energy and cyclic hardening of FCC solid solutions under multiaxial nonproportional loadings. In: *Multiaxial Fatigue and Design* (Edited by A. Pineau, G. Cailletaud and T. Lindley), E.S.I.S. 21. M.E.P., London.
12. R. C. Boettner, C. Laird and A. J. McEvily Jr. (1965) Crack nucleation and growth in high strain–low cycle fatigue. *Trans. Met. Soc. AIME* **233,** 379–387.
13. D. F. Socie, Private discussion.
14. K. Tanaka and T. Mura (1981) A dislocation model for fatigue crack initiation. *J. Appl. Mech.* **48,** 97–103.
15. H. Mughrabi (1983) A model of high-cycle fatigue-crack initiation at grain boundaries by persistent slip bands. In: *Defects, Fracture and Fatigue*, Proc of 2nd Int. Symp. Mont Gabriel, Canada, May 30–June 5, 1982 (Edited by G. C. Sih and J. W. Provan). Martinus Nijhoff Publishers, The Hague, Boston and London
16. W. Liu, M. Bayerlein, H. Mughrabi, A. Day and P. N. Quested (1992) Crystallographic features of intergranular crack initiation in fatigued copper polycrystals. *Acta Metal. Mater.* **40,** 1763–1777.
17. T. G. Zhai, S. Lin and J. M. Xiao (1990) Influence on non geometric effect of PSB on crack initiation in aluminium single crystal. *Acta Metal. Mater.* **38,** 1687–1692.
18. A. Deperrois (1991) Sur le calcul de limites d'endurance des aciers. Ph.D. Thesis, Ecole Polytechnique, Palaiseau, France.